

## Optimization of the Temperature Synthesis of Hydroxyapatite from Indonesian Crab Shells

Yazida Rizkayanti<sup>1</sup> and Yusril Yusuf<sup>1,2\*</sup>

<sup>1</sup>Department of Physics, Faculty of Mathematics and Natural Science, Universitas Gadjah Mada, Sekip Utara, Yogyakarta 55281, Indonesia.

<sup>2</sup>Nanomaterial Research Groups, Universitas Gadjah Mada, Sekip Utara, Yogyakarta 55281, Indonesia.

Received 18 May 2018; Revised 8 July 2018; Accepted 26 July 2018

### ABSTRACT

Hydroxyapatite (HAp) [ $Ca_{10}(PO_4)_6(OH)_2$ ] is a ceramic class of material widely used for medical applications. The HAp has been synthesized from Indonesian crab shells using a precipitation method at different temperatures synthesis ranging from room temperature to 80°C. The HAp was characterized using FTIR, XRD, SEM-EDS. The results demonstrate that the synthesis temperature of the HAp affected the functional groups, the phase, the crystal size, the crystallinity, the morphology, and the calcium to phosphorus ratio (Ca/P ratio). Synthesis at 80°C was identified as the optimal temperature synthesis to produce HAp from Indonesian crab shells as indicated by the crystalline pattern achieving the pure HAp by having the Ca/P ratio closest to theory (~1.67), the morphology more uniform in size, and the complete of the HAp functional group.

**Keywords:** Hydroxyapatite, Indonesian Crab Shells, Temperature Synthesis.

### 1. INTRODUCTION

Hydroxyapatite (HAp) is a ceramic class of material commonly used as a raw material in the manufacture of biomaterials for medical applications. The crystallography and chemical structure of HAp is similar to chemical constituent component of human bones and teeth. HAp can be used in dental implants, bone implants, and coating materials. HAp has a molecular formula of  $Ca_{10}(PO_4)_6(OH)_2$ . It belongs to a family of calcium phosphate compounds that has bioactive, biocompatible, and bioresorbable properties. In addition, the material made from HAp is thermally stable, so it can be used as a catalyst, an adsorbent, or a coating material. HAp can be synthesized naturally or chemically. Chemical synthesis is performed by using chemical calcium precursors, while natural synthesis uses ingredients that contain calcium, such as cow bones, eggshells, shellfish, and shell crabs.

The use of biogenic materials to produce HAp has been widely studied in the last few decades [1]. The tissue response to HAp synthesized from biogenic materials is better due to its porosity, chemistry, structural similarity to bone minerals, and easy binding to bone [2]. Biogenic materials used in the synthesis of HAp must have significant calcium levels. The shells from Indonesian crabs (rajungan) serve as good precursor material as they have a high calcium content about 66.62%. These crabs are widespread in Southeast and East Asia [3]. Based on data from the Ministry of Marine Affairs and Fisheries Republic of Indonesia in 2015, the Indonesian crab shell production is around 52,488 tons per year [4]. Generally, crab shells used

---

\* Corresponding Author: [yusril@ugm.ac.id](mailto:yusril@ugm.ac.id)

for HAp synthesis generate a large amount of environmentally-polluting waste. Therefore, a more efficient process for synthesizing HAp from biogenic materials is needed.

Several methods can be used to synthesize HAp, including the sol-gel method, the hydrothermal method and the wet chemical precipitation method [5]. However, the most suitable method for the industrial production, high purity and low cost method is the wet chemical precipitation method. It is difficult to achieve the optimal molar ratio of calcium and phosphorous (Ca/P~1.67) [6]. In order to achieve the correct Ca/P ratio, it is important to control both the pH of the HAp solution and the synthesis temperature. The pH of the HAp solution must be more than 9. Otherwise, the process will produce calcium monophosphate and calcium dihydrate. The synthesis temperature also plays a critical role. The effect of temperature on HAp synthesis has been studied by several researchers, including Zhang et al. [8], Manoj et al. [9], and Jamarun et al. [7]. Zhang *et al.* [7] reported that the physical properties of HAp are affected by synthesis conditions. Jamarun et al. [8] studied the effect of temperature on a HAp synthesis that used limestone. They found that the optimal synthesis temperature is 90°C. Lastly, Manoj et al. [9] explained that a synthesis temperature of 90°C brought about a phase change from HAp to beta tricalcium phosphate ( $\beta$  TCP).

## 2. MATERIALS AND METHODS

### 2.1 Materials

Crab shells and orthophosphoric acid ( $H_3PO_4$ ) were used as Ca and P as the precursors of hydroxyapatite. Ammonia was used to adjust the pH of the HAp solution. All reaction solutions were made with Aqua Dest distilled water.

### 2.2 Methods

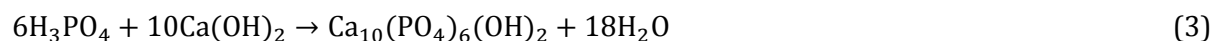
Crab shells were cleaned with Aqua Dest and dried in an oven at 100°C for three hours to isolate any contaminants. The remaining product was crushed with a ball mill for six minutes and then calcinated in a furnace at 1000°C for three hours. The calcination process converts the calcium carbonate ( $CaCO_3$ ) from the crab shells to calcium oxide ( $CaO$ ) by releasing carbon dioxide ( $CO_2$ ) as shown in Eq. (1).



HAp powders were synthesized by precipitation with calcium hydroxide ( $Ca(OH)_2$ ) and  $H_3PO_4$ . The  $Ca(OH)_2$  was created from the combination of  $CaO$  and water ( $H_2O$ ) as shown in Eq. (2).



A solution of 0.3 M  $H_3PO_4$  (85% technical grade) was mixed with a solution of 0.5 M  $Ca(OH)_2$  (Eq. 3) using a titration technique. The mixed solution was stirred for 60 minutes at room temperature or warmed to one of the following temperatures: 40°C, 60°C, and 80°C. The pH of the solution was maintained at a minimum of pH 9 by adding ammonium hydroxide ( $NH_4OH$ ). The solution was precipitated for 24 hours and then filtered with filter paper (Whatmann™ 42). The precipitate was dried at 100°C for five hours and sintered at 1000°C for three hours resulting in a HAp powder [10]. The sintering process is used in the crystallization process of HAp molecules where during sintering process the HAp molecules experience crystal growth and nucleation.



The HAp powder was characterized using FTIR at a range of  $4000\text{ cm}^{-1}$  to  $500\text{ cm}^{-1}$  to identify the functional groups. The morphology and elemental identification of the HAp powder was obtained using SEM with EDX spectroscopy. The HAp powder was also characterized using XRD to obtain phase, crystal size, and crystallinity.

### 3. RESULT AND DISCUSSION

#### 3.1 FTIR Results

The FTIR results of the HAp synthesized from crab shells at various temperatures are shown in Figure 1. Phosphate ( $\text{PO}_4^{3-}$ ) asymmetric stretching provides the first indication that HAp has been formed [7]. An asymmetric stretching vibration for  $\text{PO}_4^{3-}$  was detected in each of the temperature samples. This  $\text{PO}_4^{3-}$  vibration registered an FTIR wavenumber of  $1019\text{ cm}^{-1}$ , signifying that HAp crystals had formed [8]. However, a second  $\text{PO}_4^{3-}$  stretching vibration at wavenumber  $966\text{ cm}^{-1}$ , indicating the formation of a complete functional group, was only detected in the sample synthesized at  $80^\circ\text{C}$ .

Another indication of HAp formation can be seen in the bending vibration for  $\text{PO}_4^{3-}$  and the hydroxide ion ( $\text{OH}^-$ ). As seen in Figure 1, the  $\text{OH}^-$  was identified in all the temperature preparations at wave numbers  $621\text{ cm}^{-1}$  and  $3649\text{--}3844\text{ cm}^{-1}$ .

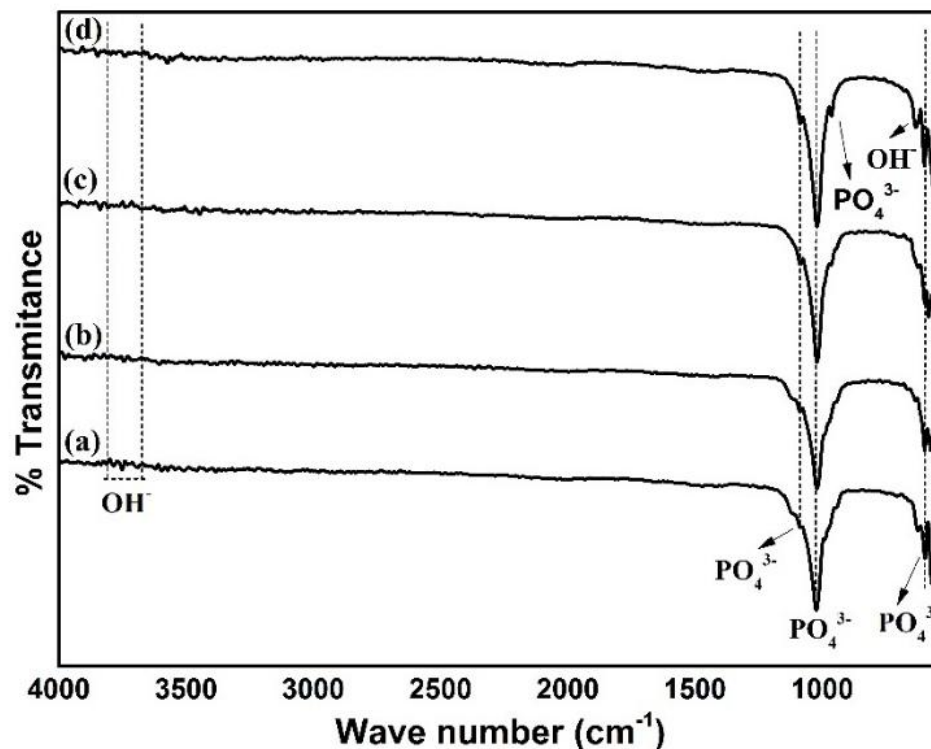


**Figure 1.** FTIR spectrum of HAp synthesized from crab shells at (a) room temperature, (b)  $40^\circ\text{C}$ , (c)  $60^\circ\text{C}$ , and (d)  $80^\circ\text{C}$ .

#### 3.2 XRD Result

FTIR results indicate HAp formation in each of the temperature samples. The FTIR results also demonstrate that the sample that was synthesized at  $80^\circ\text{C}$  has a complete functional group. The FTIR results were confirmed by XRD analysis to identify the established phases. The XRD characterization uses a Copper K- $\alpha$  ( $\lambda = 1.54060\text{ \AA}$ ) radiation source and a diffraction angle of

between 20° and 50°. The HAp diffraction peaks were matched with the Joint Committee on Powder Diffraction Standards (JCPDS) HAp data for serial number 090432 to identify the *hkl* plane of each diffraction peak. The diffraction peaks also matched with the JCPDS serial number 371497 for the CaO phase, serial number 190272 for the  $\beta$ -TCP phase, serial number 250378 for the  $H_3PO_4$  phase, and serial number 440778 for the octacalcium phosphate (OCP) phase.

The XRD patterns of HAp prepared at various temperatures are shown in Figure 2. Three higher XRD patterns of HAp have been formed, representing the *hkl* plane of HAp: (211), (112), and (300). However, XRD patterns from other phases were also identified. The XRD patterns for the HAp prepared at room temperature, 40°C, and 60°C identified the presence of phases for OCP,  $\beta$ -TCP, and  $H_3PO_4$ .

The OCP phase was identified in the samples prepared at room temperature, 40°C, and 60°C with an *hkl* plane of (610), (212), and (311). The OCP phase represents the initial phase of HAp formation. As shown in Figure 2, the intensity of the OCP phase decreases with the increase in the synthesis temperature. The OCP phase did not appear in the sample prepared at 80°C. This result is consistent with Nelson et al. who reported that the change of OCP to HAp can occur at 70°C [9,11].

Another phase that appears in the HAp samples is the  $\beta$ -TCP phase. The  $\beta$ -TCP phase, represented by the *hkl* plane (301), appears in the samples prepared at room temperature, 40°C, and 60°C. The presence of the  $\beta$ -TCP phase indicates that the  $PO_4^{3-}$  position of the crystal structure has been replaced by carbonate ions to form the following molecular formula:  $Ca_{10}(PO_4)_3(CO_3)_3(OH)_2$ . The presence of carbonate ions indicates that HAp's thermal stability has been reduced [12]. The appearance of  $\beta$ -TCP indicates that the synthesis temperature for these samples was too low. The presence of OCP and  $\beta$ -TCP in the final product is not harmful to humans because they are included in the group of apatite compounds. However, the presence of such phases may affect the thermal equilibrium and solubility of the sample [15].

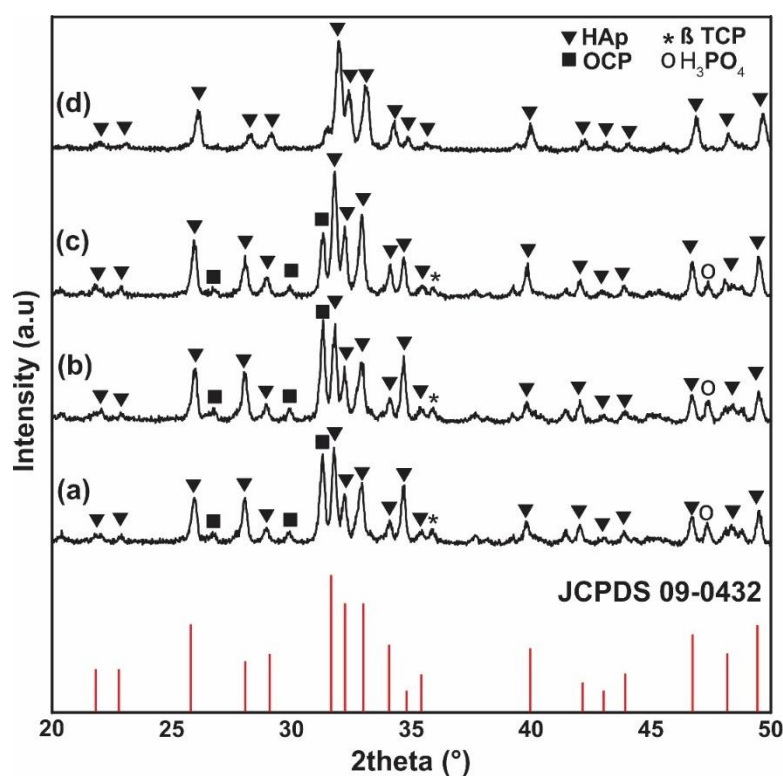


**Figure 2.** XRD patterns of HAp synthesized from crab shells at (a) room temperature, (b) 40°C, (c) 60°C, and (d) 80°C.

Another phase that was identified in the XRD patterns is the  $H_3PO_4$  phase. The presence of this phase is likely due to the residual  $H_3PO_4$  that did not react with the  $Ca(OH)_2$ . The  $H_3PO_4$  phase is not visible in the sample synthesized at  $80^\circ C$  because of the solution's efficient reaction. Increasing the synthesis temperature causes the peaks for the phase diffraction of OCP,  $\beta$ -TCP, and  $H_3PO_4$  to decrease. In the sample synthesized at  $80^\circ C$ , these peaks completely disappear. This is evidenced in an unidentified  $80^\circ C$  sample of a phase other than the HAp phase. The results of the XRD phase analysis confirmed the FTIR results. Synthesis at  $80^\circ C$  is necessary to achieve pure HAp. Furthermore, HAp synthesized at  $80^\circ C$  has a lattice parameter closest to pure HAp.

Using the Scherrer equation, the calculated crystal size of HAp is in the range of 53.43 to 71.27 nm. Several studies have reported that nano-sized HAp crystals have a greater resorbability and bioactivity than micron-sized HAp [13].

The crystallinity of HAp was calculated and the result indicates that the crystallinity increased when synthesis temperature increases. The HAp synthesized at room temperature,  $40^\circ C$ ,  $60^\circ C$  and  $80^\circ C$  have crystallinity of 57%, 58%, 67% and 75%.

### 3.3 SEM EDX Analysis

Figure 3 shows the increase in synthesis temperature resulted in HAp particles that were more uniform in size. This result is consistent with study in [14] that have uniform size occurred at  $80^\circ C$ . The higher synthesis temperature, increases the thermal vibration energy, thus accelerating the diffusion of atoms and increasing the grain size. Pang and Bao (2003) report that morphological changes of non-uniform shape to uniform shape indicate a higher degree of crystallinity [16].

SEM EDX was used to determine the Ca/P ratio of each HAp sample. The Ca/P ratio increased with the increase in synthesis temperature. The samples prepared at room temperature,  $40^\circ C$ , and  $60^\circ C$  have Ca/P ratios of 1.48, 1.41, and 1.60 respectively. These ratios correlate with the XRD results. HAp with a Ca/P ratio lower than that of pure Ca/P is not suitable for implantation, because it is too acidic. The SEM EDX results of the sample synthesized at  $80^\circ C$  have Ca/P ratios of 1.66 which is closest to pure HAp. The SEM EDX results confirmed the FTIR and XRD results. The samples that were synthesized at  $80^\circ C$  contain pure HAp.

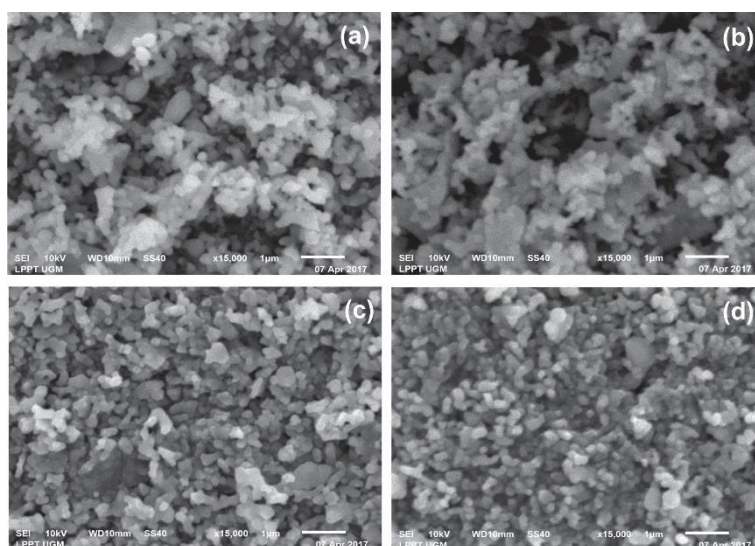


**Figure 3.** SEM EDX results of HAp synthesized from crab shells at (a) room temperature, (b)  $40^\circ C$ , (c)  $60^\circ C$ , and (d)  $80^\circ C$ .

#### 4. CONCLUSION

HAp synthesized from Indonesian crab shells is optimally prepared at 80°C. FTIR results show that synthesis at 80°C results in a more complete HAp functional group than at other temperatures. Similarly, the XRD results for the phase and lattice parameters indicate that synthesis at 80°C results in pure HAp. The SEM EDX results reveal that the HAp particles formed uniformly and that the majority of the elements are Ca, P, and O. The presence of a pure HAp phase is also confirmed by the Ca/P ratio of 1.66, which is closest to pure HAp.

#### ACKNOWLEDGMENT

The authors are immensely grateful to the Ministry of Research, Technology, and Higher Education Republic of Indonesia for financial support this research through the PUPT Grant (2456/UN1.P.III/DIT-LIT/LT/2017). The authors would also like to thank LPPT UGM for providing facilities and technical assistance.

#### REFERENCES

- [1] T. Laonapakul, "Synthesis of hydroxyapatite from biogenic wastes," *KKU Eng. J.* **42** (2015) 269–275.
- [2] R. Murugan & S. Ramakrishna, "Crystallographic Study of Hydroxyapatite Bioceramics 2005," *Crystal Growth* **5**, 1 (2005) 111–112.
- [3] J. C. Y. Lai, P. K. L. Ng & P. J. F. Davie,, "A revision of the *Portunus Pelagicus* (Linnaeus, 1758) Species Complex (Crustacea: Brachyura: Portunidae), with The Recognition of Four Species," *The Raffles Bulletin of Zoology.* **58**, 2 (2010) 199–237.
- [4] Menteri Kelautan dan Perikanan Republik Indonesia, Keputusan Menteri Kelautan Dan Perikanan Republik Indonesia, 2016. [online]. Available: <http://jdih.kkp.go.id/peraturan/70-kepmen-kp-2016-ttg-rencanapengelolaan-perikanan-rajungan.....pdf>. [Accessed: Nov. 2017].
- [5] M. R. Ayatollahi, M. Y. Yahya, H. A. Shirazi, S. A. Hasan, Abu, "Mechanical and Tribological Properties of Hydroxyapatite Nanoparticles Extracted from Natural Bovine Bone and The Bone Cement Developed by Nano-Sized Bovine Hydroxyapatite Filler," *Ceram Intl.* **41** (2015) 10818–10827.
- [6] A. Afshar, M. Ghorbani, N. Ehsani, M. R. Saeri & C. C. Sorrell, "Some Important Factors in The Wet Precipitation Process of Hydroxyapatite," *Materials&Design* **24**, 3 (2003) 197–202.
- [7] Y. Zhang & Y. Dong, "Effect of The Temperature on Synthesizing of Hydroxyapatite," *Advanced Materials Research* **914** (2014) 119–122.
- [8] N. Jamarun, Z. Azharman, S. Arief & T. P. Sari, "Effect of Temperature on Synthesis of Hydroxyapatite from Limestone," *Rasayan J. Chem.* **8**, 1 (2015) 133–137.
- [9] M. Manoj, R. Subbiah, D. Mangalaraj, N. Ponpandian, C. Viswanathan & K. Park, "Influence of Growth Parameters on the Formation of Hydroxyapatite ( HAp ) Nanostructures and Their Cell Viability Studies," *Nanobiomedicine* **2**, 2 (2015) 1–11.
- [10] F. Y. Syafaat & Y. Yusuf, "Effect of Ca:P Concentration and Calcination Temperature On Hydroxyapatite (HAp) Powders From Quail Eggshell (*Coturnix coturnix*)," *International Journal of Nanoelectronics and Materials*, **11** (2018) 51-58.
- [11] D. G. Nelson & J. D. McLean, "High-resolution electron microscopy of octacalcium phosphate and its hydrolysis products.," *Calcif. Tissue Int.* **36** (1984) 219–232.

- [12] M. Sari & Y. Yusuf, "Synthesis and Characterization of Hydroxyapatite based on Green Mussel Shells (*Perna viridis*) with Calcination Temperature Variation Using the Precipitation Method," *International Journal of Nanoelectronics and Materials*, **11**, 3 (2018) 357-370.
- [13] P. Gentile, C. J. Wilcock, C. A. Miller, R. Moorehead & P. V Hatton, "Process Optimisation to Control the Physico-Chemical Characteristics of Biomimetic Nanoscale Hydroxyapatites Prepared Using Wet Chemical Precipitation," *Materials* **8**, 5 (2015) 2297–2310.
- [14] Y. Rizkayanti & Y. Yusuf, "Effect of Temperature on Synthesis Hydroxyapatite from Cockle Shell (*Anadara Granosa*)," *International Journal of Nanoelectronics and Materials*, **11** (2018) 43-50.
- [15] Y. Rizkayanti, "Synthesis and Characterization of Hydroxyapatite (HAp) from Biogenic Material with Variation of Temperature Synthesis," Master Thesis Universitas Gadjah Mada, Indonesia, (2017).
- [16] Y. X. Pang & X. Bao, "Influence of Temperature, Ripening Time and Calcination on The Morphology and Crystallinity of Hydroxyapatite Nanoparticles," *Journal of the European Ceramic Society* **23** (2003) 1697–1704.

